

Numerical Analysis of Laminar Flow around Square Cylinders with EHD Phenomenon

M. Salmanpour, O. Nourani Zonouz

Abstract—In this research, a numerical simulation of an Electrohydrodynamic (EHD) actuator's effects on the flow around a square cylinder by using a finite volume method has been investigated. This is one of the newest ways for controlling the fluid flows. Two plate electrodes are flush-mounted on the surface of the cylinder and one wire electrode is placed on the line with zero angle of attack relative to the stagnation point and excited with DC power supply. The discharge produces an electric force and changes the local momentum behaviors in the fluid layers. For this purpose, after selecting proper domain and boundary conditions, the electric field relating to the problem has been analyzed and then the results in the form of electrical body force have been entered in the governing equations of fluid field (Navier-Stokes equations). The effect of ionic wind resulted from the Electrohydrodynamic actuator, on the velocity, pressure and the wake behind cylinder has been considered. According to the results, it is observed that the fluid flow accelerates in the nearest wall of the frontal half of the cylinder and the pressure difference between frontal and hinder cylinder is increased.

Keywords—CFD, corona discharge, electro hydrodynamics, flow around square cylinders.

I. INTRODUCTION

THE electrohydrodynamic flow is the result of the interaction between ions and the surrounding fluid molecules. This second induced flow is named as corona wind. Both electric field and fluid flow are present and interacting with each other, which makes the analysis of this phenomenon very challenging. Since several decades flow control has become a tremendous field of activity and the different ways to achieve this process have been investigated. Gad [1] did a complete research about different flow control applications. Flow control is of immense technological importance for industry where internal and external airflows occur, and more especially for aeronautics. The huge potential application for several industrial processes involving dielectric liquids like oil in transformers, high temperature cooling system or fuel injection in gas turbine justify the effort of the scientific community in this area. EHD actuators mainly consist in using the injection-induced ionic stream within the boundary layer to modify its properties and then to actively manipulate the flow. One of the undesirable phenomenon's in flow field is flow separation. The main result of EHD method

is to construct a tangential flow near the solid boundary which makes the velocity distribution through the viscous boundary layer more powerful and transition of the flow regime happened more rapidly. The final goal is to prevent or in the contrary according to the objective to induce the boundary layer separation. Meanwhile, because the EHD flow is generated without any mechanical moving parts and the electrical energy is converted directly to the mechanical energy in the process, it finds numerous potential applications. Hauksbee [2] found the ionic wind which named as corona wind for the first time. Yabe, Mori, and Hijikata [3] experimentally studied the corona wind between wire and plate electrode and they measured spatial distribution of ions. Ohadi, Nelson and Zia [4] found that the enhancement effect of the ionic wind is significant only in laminar and transition regimes when using a single wire electrode in a pipe flow, but also it is extended to turbulent flow regime by using two wire electrode arrangements. Leger, Moreau and Touchard [5] analyzed the ability of a DC electrical discharge to control low velocity air flow along a flat plate. They showed that the ionic wind induced by the corona discharge modifies the original airflow considerably, resulting in the air flow reattachment to the wall and reduction of the wake size.

II. FORMULATION OF PROBLEM

Fig. 1 shows the geometry of problem which includes a cylinder with $0.034\text{ m} \times 0.034\text{ m}$ cross section. The air cross flow is considered as a steady two dimensional flow. Two types of electrodes are used in this work: Two planar electrodes which are flush-mounted on the up and down surfaces of the cylinder and one wire electrode which is placed on the line with zero angle of attack relative to the stagnation point and excited with DC power supply. The positions of electrodes are shown in Fig. 1. When the Reynolds number is lower than the critical value for this given flow around a square cylinder, the flow structure is made of two main stationary vortices attached on the back of the cylinder. The critical value of the Reynolds number above which the vortex shedding start to evolve is known to be around 55 [6], [7]. Above this critical value vortex shedding starts, giving rise to the well-known Von Karman Street due to the development of the Kelvin-Helmoltz instability. The selected Reynolds number in this research is lower than the critical value.

M. Salmanpour is with Department of Mechanical Engineering, College of Engineering, Marvdasht Branch, Islamic Azad University, Marvdasht, Iran (phone: +98-915-310-2637; fax: +98-711-6347853; e-mail: Salmanpoumehdi@gmail.com).

O. Nourani Zonouz is with Department of Mechanical Engineering, College of Engineering, Marvdasht Branch, Islamic Azad University, Marvdasht, Iran (e-mail:ouldouzn@gmail.com).

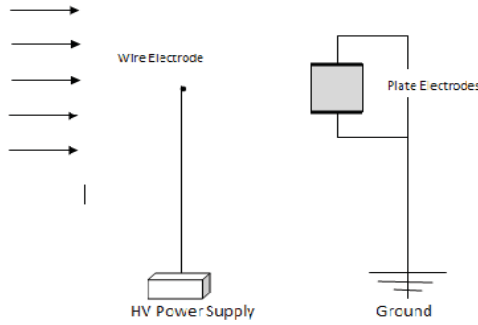


Fig. 1 The positions of electrodes

III. GOVERNING EQUATIONS

The problem is formulated considering the usual hypotheses of a Newtonian and incompressible fluid of kinematic viscosity ν , density ρ . The following governing equations are listed in non-dimensional form:

$$\nabla \cdot \mathbf{U} = 0 \tag{1}$$

$$(\mathbf{U} \cdot \nabla) \mathbf{U} = -\nabla P + \frac{1}{Re} \Delta \mathbf{U} + CM^2 R^2 q \mathbf{E} \tag{2}$$

$$\nabla \cdot (q(\mathbf{U} + R\mathbf{E})) = 0 \tag{3}$$

$$\Delta V = -Cq \tag{4}$$

$$\mathbf{E} = -\nabla V \tag{5}$$

where \mathbf{U} is the fluid velocity, P the pressure, q the charge density, V the potential and \mathbf{E} the electric field. The reference length and velocity are the diameter of cross section and U_∞ . The produced non-dimensional group numbers are as follows:

$$T = \frac{\epsilon \Delta V}{\rho \nu K}, C = \frac{q_0 H^2}{\epsilon \Delta V}, M^2 = \frac{\epsilon}{\rho K^2}, R = T/M^2$$

T is the parameter which accounts the potential difference, C is a measure of the injection level, M is the mobility parameter, R is Electrical Reynolds number, K is the ionic mobility, ϵ the permittivity and q_0 the local injected charge.

The selected Reynolds numbers are between 11 and 35 which are lower than critical value. The normal direction gradients of all parameters in up and down boundaries are zero. In this work the electrode potential on the wire electrode was 10 and 15 kV and the plate electrodes were ground electrodes.

IV. RESULTS

The entire set of conservation equations include mass; momentum, charge and potential are solved directly. The electrodynamic equations coupled with the Navier-Stokes equations are solved numerically using finite volume method [8]. Some additional features on the numerical method can be found in [9]-[11]. Figs. 2-4 demonstrate the horizontal component velocity at $L/2, 3L/2, 2L$ and $5L/2$ positions according to the beginning of the body. L is the length of the square side. In Figs. 5-7, the vertical component of velocity in

same positions is shown. These figures clearly present the trend of the velocity distribution in back of the cylinder.

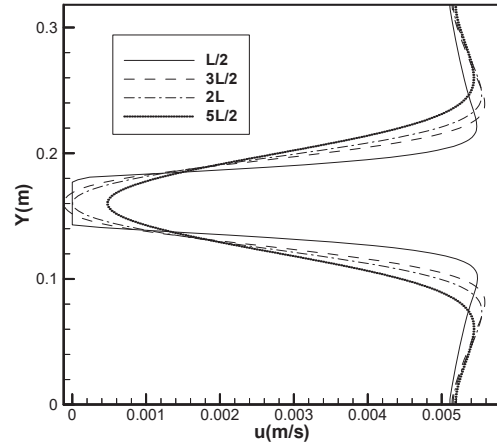


Fig. 2 Velocity distribution (horizontal component) in wake region (Re=11)

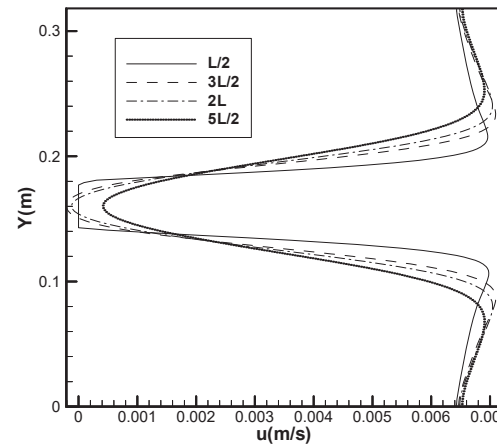


Fig. 3 Velocity distribution (horizontal component) in wake region (Re=14)

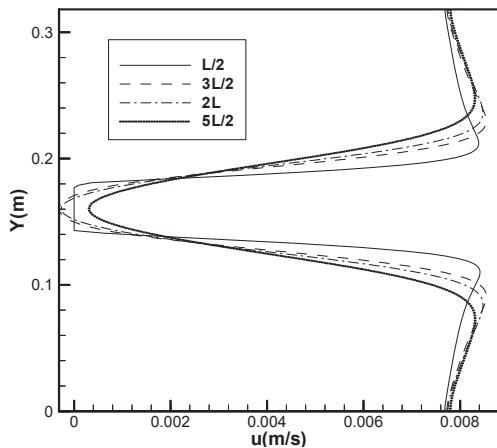


Fig. 4 Velocity distribution (horizontal component) in wake region (Re=17)

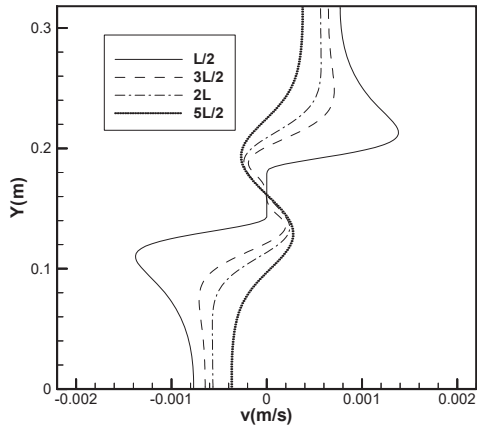


Fig. 5 Velocity distribution (vertical component) in wake region (Re=11)

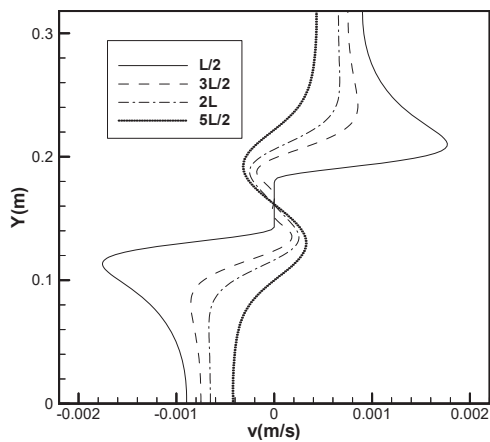


Fig. 6 Velocity distribution (vertical component) in wake region (Re=14)

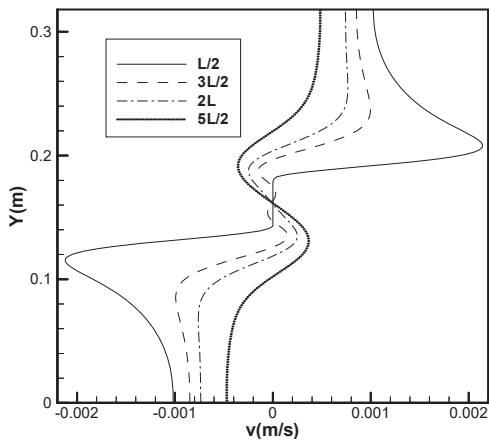


Fig. 7 Velocity distribution (vertical component) in wake region (Re=17)

shows that wire electrode has the maximum value of electrical field intensity and this value finds zero on the ground wire.

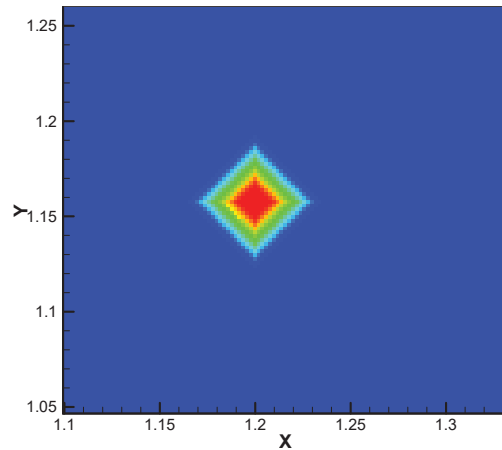


Fig. 8 Electrical density distribution around the wire electrode (Vol=10 kv)

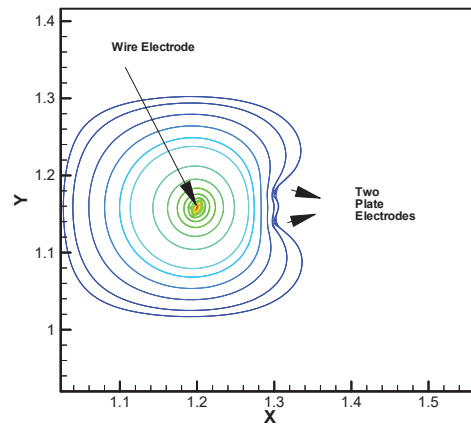


Fig. 9 Voltage distribution around the wire and plate electrode (Vol=10 kv)

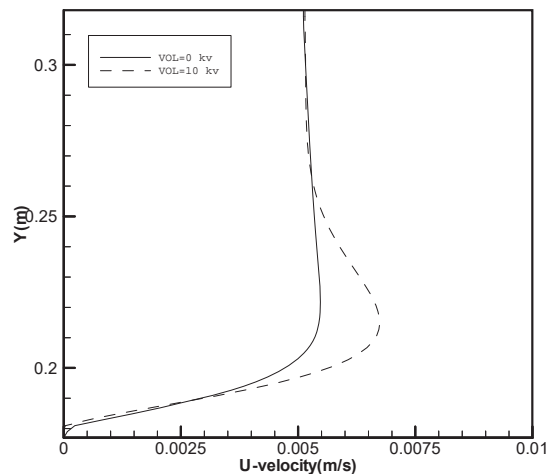


Fig. 10 Velocity profile over the center surface of the cylinder (Re=11)

Fig. 8 demonstrates the electrical density contour around the wire electrode. The magnitude of the density decreased sharply in far fields. In Fig. 9 the contour of electrical field around the wire and plate electrodes are sketched. The result

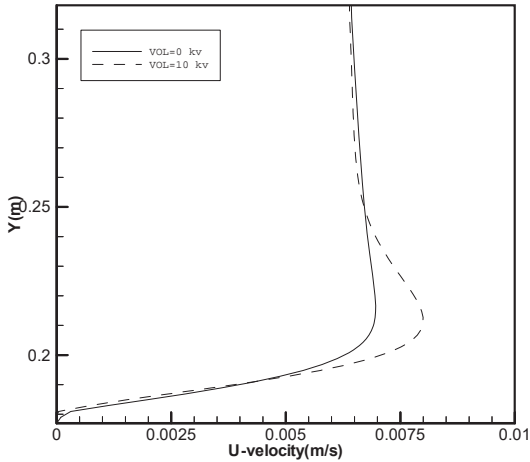


Fig. 11 Velocity profile over the center surface of the cylinder (Re=14)

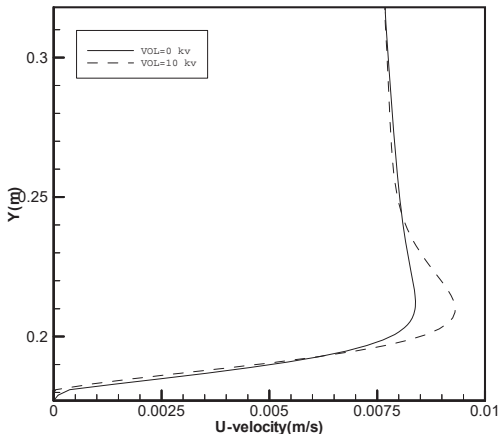


Fig. 12 Velocity profile over the center surface of the cylinder (Re=17)

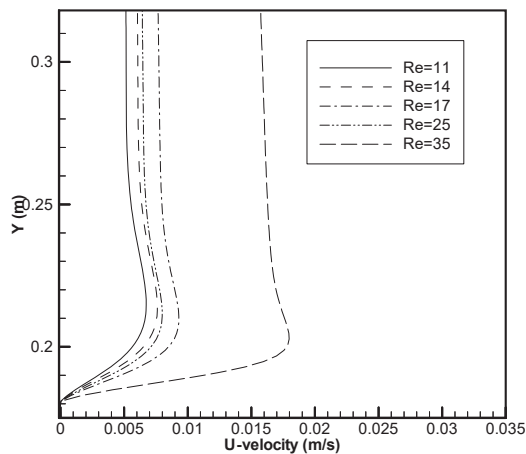


Fig. 13 Velocity profile over the center surface of the cylinder for difference Reynolds numbers (10 kv)

With inducing the EHD phenomenon through the flow field, the power of the flow (momentum flux) will be

increased. In Figs. 10-13, the velocity profile for different Reynolds number in a same position is shown. The trend of these graphs tells us that the EHD phenomenon makes these profiles thicker.

In low Reynolds number the EHD phenomenon is more effective. Figs. 14 and 15 show us the velocity profile for 3 cases: VOL=0, 10 and 15 KV for two Reynolds numbers 11 and 35. Comparing these two figures tells us that EHD phenomenon in smaller Reynolds number (Re=11) makes the velocity profile thicker.

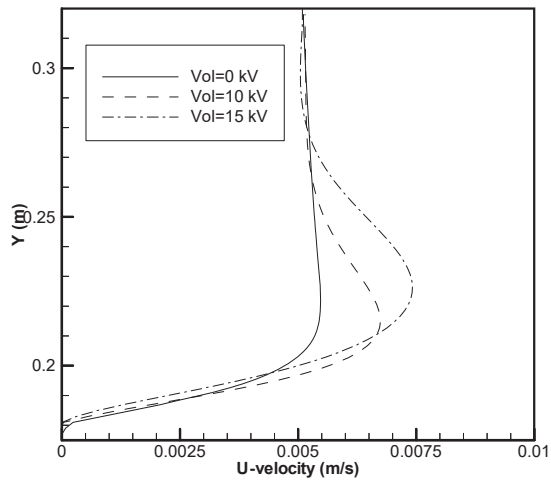


Fig. 14 Velocity profile over the center surface of the cylinder (Re=11)

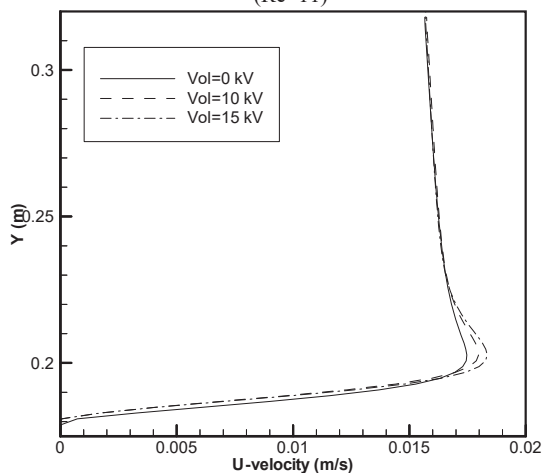


Fig. 15 Velocity profile over the center surface of the cylinder (Re=35)

In most flow fields around the immersed bodies, separation will be happened. The wake region produced in the back of the body is the most side effect of this phenomenon. In turbulence flows the wake is smaller than the laminar fields. With changing the regime of the flow, the side effect of the separation will be diminished. The effect of the EHD phenomenon is alike the changing the regime of the flow field. Fig. 16 shows us the length of recirculation zone for different Reynolds numbers. By increasing the voltage, the length of the

recirculation zone will be increased, which means that the wake will be thinner.

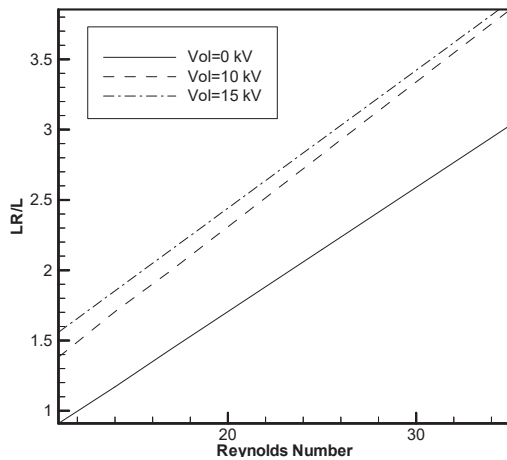


Fig. 16 Recirculation length for different Reynolds numbers

LR is the recirculation length and L is the length of the square side. One of the important parameters in flow fields is pressure coefficient (cp). Fig. 17 shows the trend of cp around the cylinder. The absolute of this parameter will be increased by inducing the electrical field to the main flow field.

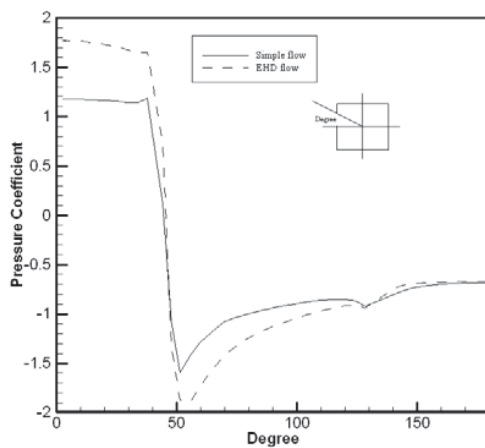


Fig. 17 Pressure coefficient around the cylinder for (Re=14)

V. CONCLUSIONS

The present work aims to explore the Electrohydrodynamic actuator's effects on the flow around a square cylinder by using a finite volume method. The discharge produces an electric force and changes the local momentum behaviors in the fluid layers. The effect of ionic wind resulted from the Electrohydrodynamic actuator, accelerates airflow near the wire electrode, therefore airflow reaches to the cylinder more rapidly. This ascend of flow velocity causes the pressure increases in front of the cylinder, hence the pressure coefficient will be increased in this region. The more voltage difference increases, the more pressure coefficient gets positive values. The effect of hydrodynamic phenomena at the

behind of the cylinder is less than the front region. According to the results, it is observed that the fluid flow accelerates in the nearest wall of the frontal half of the cylinder and the pressure difference between frontal and hinder cylinder is increased. When a voltage difference applied, the flow momentum near the wall of the cylinder enhanced and the velocity profile modified.

REFERENCES

- [1] M. Gad el Hak, "Modern developments in flow control" *Applied Mechanics Reviews*, Vol.49, 1996, pp. 365-379.
- [2] F. Hauksbee, "Physico-Mechanical Experiments on Various Subjects" 1719, pp. 46-47.
- [3] A. Yabe, Y. Mori, and K. Hijikata, "EHD study of the corona wind between wire and plate electrode" *AIAA Journal*, Vol.16, No.4, 1978, pp. 340-345.
- [4] M. Ohadi, D.A. Nelson and S. Zia, "Heat Transfer Enhancement of Laminar and Turbulent Pipe Flow via Corona Discharge" *Inter. Journal of Heat and Mass Transfer*, Vol. 34, 1991, pp.1175-1187.
- [5] L. Leger, E. Moreau and G. Touchard, "Effect of a DC corona electrical discharge on the air flow along a flat plate". *IEEE Transactions on industry application*, Vol. 38, No.6, 2002, pp.1478-1485.
- [6] A. Sohankar, C. Norberg, L. Davidson, "Low Reynolds number flow around a square cylinder at incidence: study of blockage, onset of vortex shedding and outlet boundary condition" *Int. J. Numerical Methods in Fluids*, Vol.26, 1998, pp. 39-56.
- [7] A. Sohankar, C. Norberg, L. Davidson, "Simulation of three-dimensional flow around a square cylinder at moderate Reynolds numbers". *Phys. Fluids*, Vol. 11, 1999, pp. 288-305.
- [8] S. Patankar, "Numerical Heat Transfer and Fluid Flow". *Stockholm, Washington, DC*, 1980.
- [9] A. T. Perez, Ph. Traoré , D. Koulova , H. Romat , "Numerical Modeling of a Two-Dimensional Electrohydrodynamic Plume between a Blade and a Flat Plate". *16th International Conference on Dielectric Liquids*, Poitiers, 2008, pp. 44-47.
- [10] Ph. Traoré, A.T. Pérez, D. Koulova-Nenova, H. Romat, "Numerical modelling of finite amplitude electro-thermo-convection in a dielectric liquid layer subjected to both unipolar injection and temperature gradient". *Journal of Fluid Mechanics*, No. 658, 2010, pp. 279-293.